Hindawi
Journal of Robotics
Volume 2022, Article ID 2576303, 11 pages
https://doi.org/10.1155/2022/2576303

Research Article

Research and Implementation of Turbo Coding Technology in High-Speed Underwater Acoustic OFDM Communication

Yarang Yang[1] **and Yunpeng Li**[2]

[1]*College of Physics and Electrical Engineering, Kashi University, Kashi, Xinjiang 844006, China*
[2]*Qingdao Vocational and Technical College of Hotel Management, Qingdao, Shandong 266100, China*

Correspondence should be addressed to Yunpeng Li; liyunpeng@qchm.edu.cn

Received 28 December 2021; Accepted 17 February 2022; Published 15 March 2022

Academic Editor: Shan Zhong

It is demonstrated that the fully parallel turbo decoding algorithm can achieve an approximate error correction decoding performance when 36 iterations are used and when the log-map algorithm with 6 iterations is used. By comparison, it is shown that it can achieve much higher decoding rates than the log-map algorithm for various frame lengths of LTE standard turbo codes at the cost of higher hardware resource requirements. According to the fully parallel turbo decoding algorithm, this paper proposes a scheme for implementing a fully parallel turbo decoder on FPGA, detailing the overall structure and processing of the decoder hardware implementation, the design of the algorithm block processing unit, and the interleaving module. The performance of the decoder is tested by fixed-point simulation for different frame lengths of turbo coding in LTE standard, and it is proved that the fully parallel turbo decoder can be applied to turbo coding of various frame lengths. Both simulation and experimental results show that the distributed cancellation method and the joint estimation cancellation method have good results for both time-domain impulse noise and large-amplitude single frequency noise cancellation, while the joint estimation cancellation method of large-amplitude single frequency noise cancellation first has better performance.

1. Introduction

Hydroacoustic communication is a rapidly developing field of scientific research; its engineering applications used to be limited to military aspects to solve the problem of mine remote control, submarine to submarine, mother ship and submarine, or other underwater unmanned combat platform transmissions to obtain battlefield information, and limited bandwidth, multipath, transmission delay, and channel structure of the rapid time change are currently difficult problems [1].

After years of development, OFDM has fully demonstrated its advantages, but some problems based on the hydroacoustic OFDM communication system are still not well solved. Many communication methods are controversial, there is no unified standard, and different experiments are usually used in different system parameters, such as coding modulation, communication bandwidth, and carrier frequency. The problems in hydroacoustic OFDM communication need to be studied in more depth, such as how to eliminate external noise interference; how to eliminate and compensate the impact of UAC on the OFDM system to ensure high system reliability; how to better use the sparsity characteristics of UAC to improve system performance; how to adapt to the hydroacoustic communication channel by using coding techniques to improve system performance; and how to improve the utilization of frequency band to achieve high-speed hydroacoustic communication.

The hydroacoustic channel is very complex, with strong multipath and complex noise interference, and the channel parameters are time varying, so it is very difficult to get the state information of the hydroacoustic channel at the transmitter side. The transmitter side achieves adaptive transmission based on the obtained CSI, but the hydroacoustic channel is time varying and there is a certain delay

in the process of feeding CSI back to the transmitter side. Therefore, this paper investigates the prediction of hydroacoustic channels based on the OFDM system and proposes a channel prediction technique based on the sparsity of hydroacoustic channels to compensate for the time delay of underwater transmission, so that the obtained channel state information can better reflect the current channel condition. Because of the channel characteristics such as space-time frequency variation and narrow-band, high-noise, strong multipath interference, and large transmission delay, Turbo codes combine convolutional codes and random interleavers to realize the idea of random coding, while soft-output iterative decoding is used to approximate the maximum likelihood decoding, which can help achieve the channel coding performance limited by Shannon theory over Gaussian channels [2, 3].

2. Key Technologies for High-Speed Hydroacoustic Communication

The key technologies for high-speed hydroacoustic communications include six main directions, namely, new modulation methods to reduce the effects of multipath; coding techniques, including compression coding required for image transmission and error correction coding techniques that can improve system reliability; receiver architecture, as reflected in the use of powerful signal processors and algorithms; underwater network systems; various explicit and implicit diversity techniques applied to fading channels; and hydroacoustic channel physics. The topics include the simulation and measurement of channels [2].

After decades of development, the hydroacoustic communication method has gradually tended to move from noncoherent communication to coherent communication, with new technologies and advances in signal modulation and demodulation and signal processing, such as spatial modulation technology and blind equalization technology. According to historical materials, it was Leonardo da Vinci who pioneered a method of transmitting and receiving information underwater, which can be traced back to the earliest hydroacoustic communication system. Several frequency points are selected in the frequency band, and the transmission of information works at the transmitting end by transmitting carriers of different frequencies. The frequency shift keying system is more stable than the ASK system communication performance, but the same communication rate is slower, and the frequency band utilization is not high, the information of adjacent frequency points is easily affected by Doppler shift, and the demodulation is easy to generate false codes.

Multipath propagation causes intercode interference in single-carrier digital communication systems, introduces multipath expansion between symbols, and to some extent limits the use of single-carrier communication technology for high-speed hydroacoustic communication systems. In shallow sea channels, the time-varying nature of the seawater medium and the relative motion between the transmitter and receiver are the two factors that cause Doppler frequency shift. The application of OFDM communication technology to hydroacoustic communication requires overcoming the Doppler shift. Due to the above complex characteristics of the shallow sea hydroacoustic channel, various OFDM-based communication technologies must be improved accordingly to apply to the hydroacoustic channel, and a lot of experimental validation is needed after the improvement to be put into use.

3. OFDM for Hydroacoustic Communication Systems

3.1. OFDM for Hydroacoustic Communication Systems. The basic principle of OFDM is to split the original signal into N subsignals by serial-parallel conversion: if the serial code rate is R, the converted code rate is R/N, the subsignal period is Δt, and the theoretical value of the complete period of the original signal is $T = N * \Delta t$. Then the N subsignals are modulated on N mutually orthogonal subcarriers, and finally the N modulated signals are summed to get the transmit signal. At the receiving end, the input signal is divided into N branches, and then the N subcarriers are mixed and integrated to recover the original data. At the receiving end, the input signal is divided into N branches, which are mixed and integrated with N subcarriers to recover the parallel data, and then the original data can be recovered through parallel-serial conversion and demodulation [4].

$$\left[T_1 - T_{\min} + k \cdot T\right] < T_2 + \Delta t < \left[T_1 + T_{\min} + (k+1) \cdot T\right]. \tag{1}$$

The phenomenon of self-interference exists in the hydroacoustic communication system, that is, the signal sent by a terminal after mechanical vibration and another short-range low-attenuation propagation method to reach its receiving transducer, and its amplitude is much larger than the target signal propagated from other terminals over long distances. Therefore, the frequency division multiplexing of the hydroacoustic system in the simultaneous transmission and reception of signals, the need to filter out the self-interference signal, and the system's filtering performance put forward high requirements, and engineering implementation is also more difficult; time-division multiplexing system in the reception of signals also needs to send a signal after a certain interval, waiting for the elimination of the self-interference component before collecting data.

$$T_2 + \Delta t \le \left[T_1 + T_{\min} + k \cdot T\right]. \tag{2}$$

Different terminals have different requirements for communication indicators, which include communication type, communication target, communication speed, and communication delay. Take an exploration activity that includes a diver, an underwater probe, an underwater beacon, and a mother ship as an example: the diver and the mother ship communicate with each other through commands, and the mother ship sends commands to the diver to direct him to conduct underwater exploration. This process requires a small communication delay; the underwater probe sends data back to the mother ship in one direction, which

does not require high communication delay, but high communication speed; the underwater beacon sends commands back to the mother ship in one direction, which requires high real-time communication and does not require high communication speed.

$$v_0 = \frac{k \cdot T}{2\left[T_1 + T_{\max} + (k+1) \cdot T - 2\Delta t\right]},$$
$$a = A\frac{Sf_r f^2}{f_r^2 - f^2} - B\frac{f^2}{f}. \tag{3}$$

The overlapping time slot allocation method is still applied under the condition that the propagation time of the acoustic signal is greater than the minimum time slot. The first time slot is allocated for the host and the slave to send signals simultaneously, while the second time slot is allocated for the host and the slave to receive signals simultaneously. When communication is performed in this way, the highest communication rate per unit time is achieved because as many data frames as possible are transmitted, but the communication delay of the system is larger. If the host or slave needs to send data at moment t, the earliest it can receive this signal is at moment $3t$, and the longest communication delay is twice the propagation time.

3.2. Key Technologies of a Hydroacoustic Communication System with OFDM. The key technologies of OFDM's hydroacoustic communication system mainly include spatial diversity.

$$\psi(t) = \exp\left(j\lambda t + \gamma t^a - j\beta \operatorname{sgn}(t)\varphi(t,a)\right),$$
$$\varphi(t,a) = \begin{cases} \tan\left(\dfrac{a\pi}{3}\right), & a \neq 1, \\ \ln t, & a = 1. \end{cases} \tag{4}$$

Having$\lambda, \gamma, \alpha, \beta$ as four parameters, the characteristic function of the steady-state distribution can be obtained by these four parameters. The accurate measurement of the pressure expansion ratio of the signal effectively compensates for the Doppler of the signal, while the compensation of the consistent Doppler frequency bias is usually required again after the variable sampling due to the measurement and compensation accuracy.

Compared with single-carrier systems, OFDM signals behave in the time domain as a superposition of N mutually orthogonal subcarrier signals. When all these N signals are exactly summed at the peak point, the OFDM signal produces the maximum peak, which is N times the average power, and the peak-to-average power ratio is correspondingly larger. As the number of subcarriers N increases, the maximum value of peak-to-average power ratio (PAPR) also increases linearly, which puts high requirements on the linear range of the transmitter front-end amplifier, so a simple and effective technique to reduce the peak-to-average power ratio becomes an important research direction for OFDM technology.

$$h(t,\tau) = \sum_{p=1}^{N_{pa}} \xi_p(t)\delta\left(\tau + \tau_p(t)\right), \tag{5}$$

where N denotes the number of paths, $\tau_p(t)$ denotes the amplitude of the path, and $\xi_p(t)$ denotes the delay of the amplitude of the path. Coherent communication of hydroacoustic communication systems must perform channel estimation and compensation for correct demodulation. Using hydroacoustic channel characteristics, such as the sparse nature of the channel, the design of a simple structure, low computation, and high estimation accuracy of the channel estimation, an equalization algorithm is a key technology for multicarrier hydroacoustic communications.

As much as possible, the bits in the information sequence input to the interleaver are disordered so that the information bits nearby before interleaving are permuted to positions farther apart after interleaving, especially not to have information bits that are originally adjacent to each other still in adjacent positions after being permuted. Try not to have the bits in the information sequence of an input interleaved, after being permuted by the interleaver and when it does not go through interleaving, corresponding to the check bits in the output check sequence of different component encoders that are most correlated with it and are in the position where the censoring operation will be performed. The theory of ray propagation is expounded, and, on this basis, the sound ray span model and the search algorithm for eigenrays in the layered ocean based on the model are introduced. The algorithm can quickly and accurately search for important eigenrays. Then, the eigenpath model of the underwater acoustic channel is given in this paper, and the eigenpath channel is analyzed in detail with mathematical formulas from the aspects of propagation attenuation and delay, multipath components, and Doppler frequency shift, along with the rationality and feasibility of the model. The length of the interleave is increased as much as possible so that the correlation of the information sequence before and after interleaving is as low as possible, thus obtaining a turbo coded output sequence with a larger minimum Hamming distance and a minimum Hamming distance code word, which can reach a lower BER limit.

In the practical application of communication systems, the choice of interleaver used in turbo encoder requires a balance between the error correction decoding performance and the complexity it requires for hardware implementation. In the LTE standard, a quadratic permutation polynomial interleaved is chosen for turbo coding. The redundant bits can be removed by the redundancy process because the conventional turbo encoder uses two fractional convolutional encoders to obtain two sequences of check bits equal to the length of the information bit sequence as the redundant bits of the coded output, which is twice as many as the check bits needed in general, and this extra check bits can be removed by the redundancy process, which can reduce the redundancy of the turbo coded output sequence and obtain higher performance. These extra parity bits can be removed through redundancy processing, thus reducing the

redundancy of the turbo coding output sequence and obtaining a higher code rate.

3.3. Advantages and Disadvantages of a Hydroacoustic Communication System with OFDM. The advantages of the OFDM system are strong resistance to intercode interference, suitability for high-speed data transmission, high-frequency utilization, and strong antifading ability. OFDM is strong against intercode interference due to the use of cyclic prefix [5].

The shortcomings of OFDM technology include sensitivity to frequency bias and phase noise and large power peak-to-mean ratio. The power efficiency of the OFDM signal is lower, and the OFDM signal is summed by multiple independent modulated subcarrier signals [6].

4. Turbo Code-Based High-Speed Hydroacoustic OFDM Communication Coding Scheme Design

4.1. High-Speed Hydroacoustic OFDM-Based Communication System Structure Design. The architecture of the high-speed hydroacoustic OFDM-based communication system shown in Figure 1 includes coding, interleaving, and modulation modules.

High-speed hydroacoustic OFDM-based communication system architecture support all mandatory and optional data rates: 6, 9, 12, 18, 24, 36, 48, and 54 Mb/s, including adaptive modulation and multipath fading channel dispersion, i.e., simulating dynamically changing data rates encoded with a high channel fading rate and allowing data rates to change more rapidly, and random data generation at a bit rate simulates a variety of code rate environments that hold at different data rates for some time so that the required data rate depends on the expected value of the module; it uses 1/2, 2/3, and 3/4 convolutional coding code rates, uses data interleaving design, and supports BPSK, QPSK modulation, 16QAM, and 64QAM modulation [7]. See Figure 2 for an OFDM frame fusion module based on the architecture of a high-speed hydroacoustic OFDM communication system.

The high-speed hydroacoustic OFDM-based communication system architecture corrects the number of data symbols and omitted bits in each packet and uses an uninterrupted frame structure, omitting the tail part; the decoder has a reset state and fixes the transmit power level instead of the average signal-to-noise ratio of the different channels.

In general, a high input SNR implies a high output SNR and a high prediction accuracy. However, the length of the cyclic prefix determines the size of the input SNR. If the cyclic prefix is too long, fewer noise coefficients will be removed and the accuracy of the time-domain channel prediction will be affected. If the cyclic prefix is too short, it will make the actual channel tap coefficients potentially leaky and lead to a serious loss of prediction performance [8–11]. Therefore, in time domain channel prediction, choosing the appropriate length of the cyclic prefix has a certain impact on the improvement of the prediction performance.

The Turbo frequency domain equalizer structure is shown in Figure 3. Both demodulator and decoder use processing operates a priori on the input and output values, providing a Turbo excitation for the next iteration. The same Turbo processing principles apply to coded CDMA systems, producing Turbo multiuser detection.

Amplifier circuits are divided into Class A, Class B, Class A-B, and Class *D* according to their efficiency, of which Class A amplifiers have an amplifier tube conduction angle of 360°. Class B amplifiers have a conduction angle of 180°; the amplifier tube only works in half a cycle and can only amplify the positive half-cycle signal [12–14]. Raised cosine filters (also known as Nyquist filters) generate bandwidth-limited signals without intermember interference, making them the most commonly used filter type for OFDM modulation. In most communication systems, the raised cosine overall response is obtained by evenly distributing the filtering between the transmitter and receiver, resulting in a square root raised cosine filter. For the OFDM modulation scheme, where the amplitude is constant and the data being transmitted are used to control the carrier frequency, a Gaussian filter is typically used to modulate the signal (rather than the RF signal). The common push-pull amplification structure is the use of two amplifier tube combinations, respectively, amplifying the positive and negative half-cycle signal and then synthesizing as the output. Class A and B amplifiers are slightly less efficient than class B amplifiers, but they solve the problem of crossover distortion of class B push-pull amplification. Class *D* amplifier tube is switching, and the efficiency is very high, but the circuit design and impedance matching are very tedious and easy to lead to signal nonlinear distortion. This system selects the high-efficiency Class A and B amplifier structure to build the power amplifier circuit.

4.2. Design of Turbo Code Coding Scheme in the High-Speed Hydroacoustic OFDM Communication. The original coding structure of the Turbo code encoder is Parallel Concatenated Convolution Codes (PCCC), as shown in Figure 4 [8], which cleverly combines convolutional codes and random interleavers to realize random coding while constructing long codes from short codes through the interleaved.

The Turbo code has a much better error correction decoding performance than traditional channel coding schemes such as packet codes and convolutional codes because, on the one hand, the interleave is used to obtain two check sequences with low correlation as the coding output and, on the other hand, the decoder uses an iterative decoding method by exchanging soft information between the component decoders. Since a hard decision will lose some information in the information sequence, the decoder uses two soft-input and soft-output component decoders to preserve as much as possible the information of the system information sequence contained in the different check sequences.

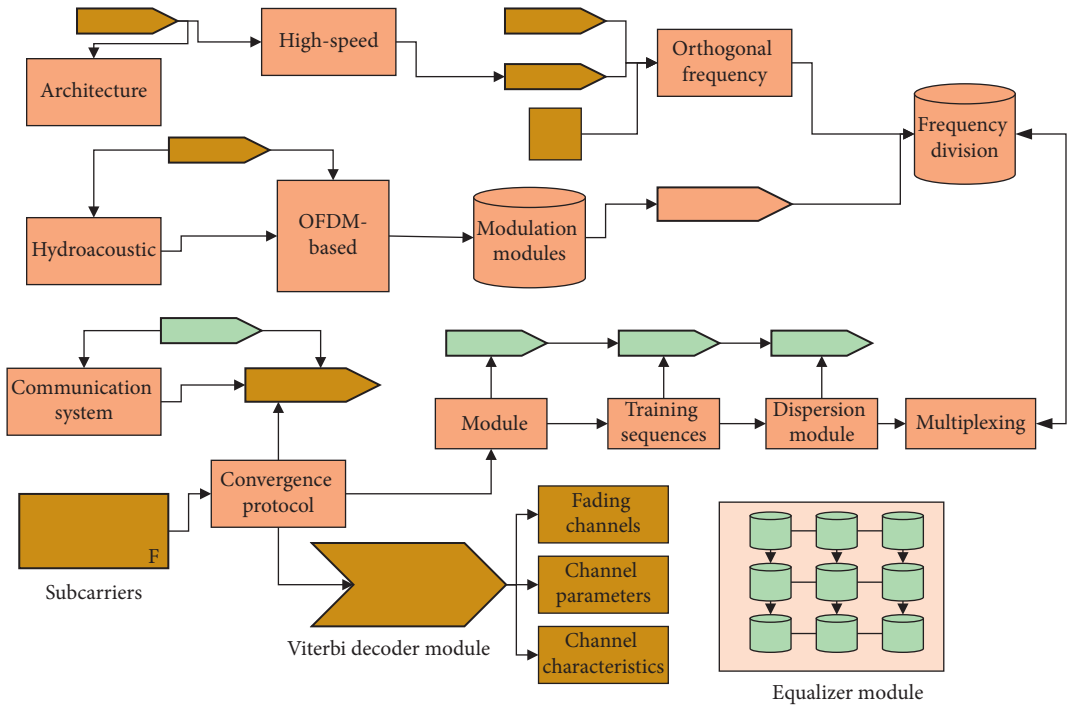

Figure 1: Structure of high-speed hydroacoustic OFDM-based communication system.

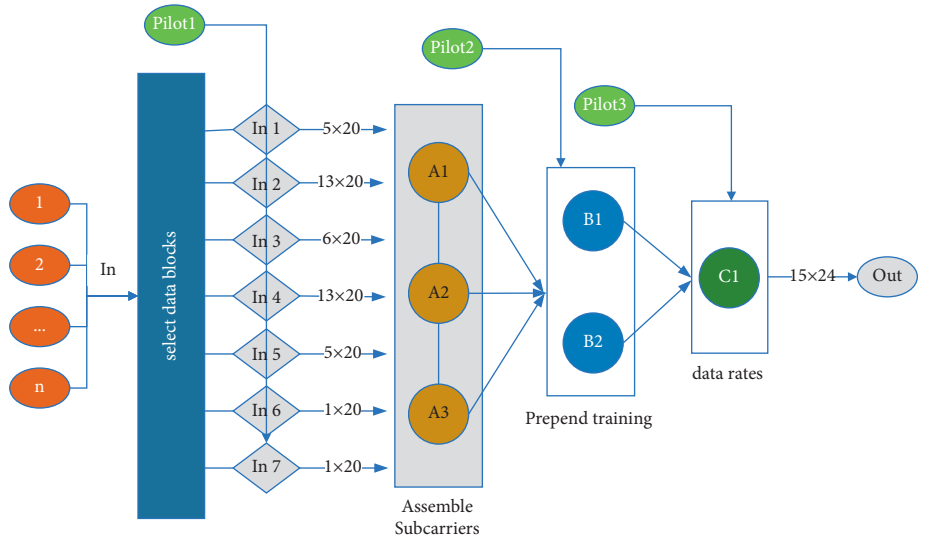

Figure 2: OFDM frame fusion module based on the structure of high-speed hydroacoustic OFDM communication system.

Since the output of the two ends of the receiver transducer is a differential signal with a DC bias, direct amplification of this differential signal with an uncertain reference level tends to overload the input of the amplifier circuit [15]. The error of our simulation and experimental results is small, less than 1%, which can illustrate the accuracy of our theory. Therefore, a differential to single-ended amplifier circuit is introduced to convert the differential signal into a single-ended signal whose reference level is the ground level in the circuit for poststage processing. The differential to single-ended circuit also suppresses the common-mode component of the output signal of the hydroacoustic transducer. The differential amplifier circuit is built using TI's low-power instrumentation amplifier INA118.

As shown in Figure 5, the Turbo encoder is usually designed to consist of two or more conventional decoders connected in parallel. To ensure that the data received by the encoder is statistically independent, an interleaver is added between the two conventional decoders.

The same is fed to the convolutional encoder in bit format. This encoder obtains this data, ready to be sent over the physical channel, by competing for information,

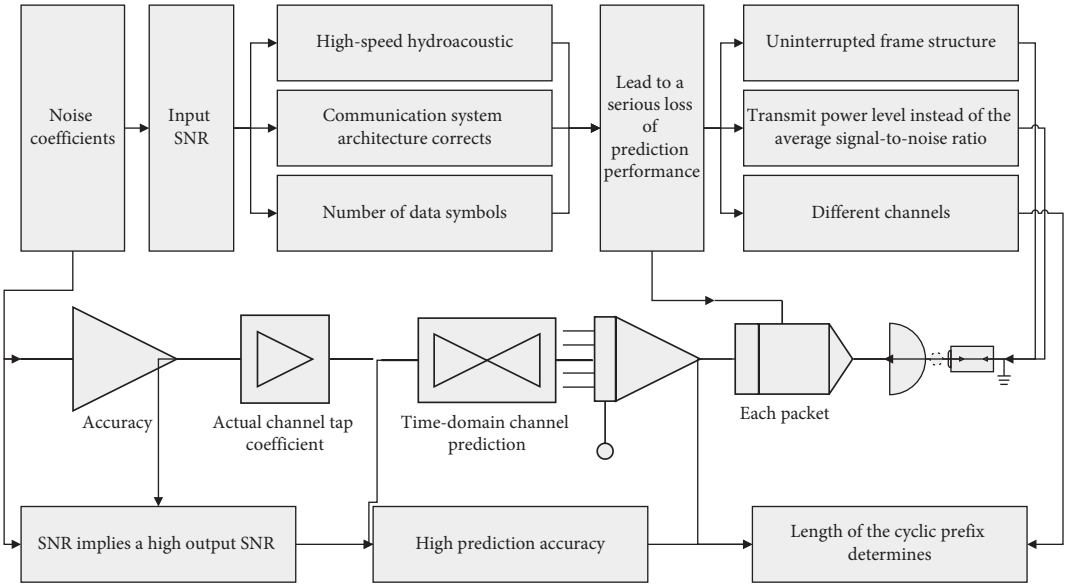

Figure 3: Frequency domain equalizer structure.

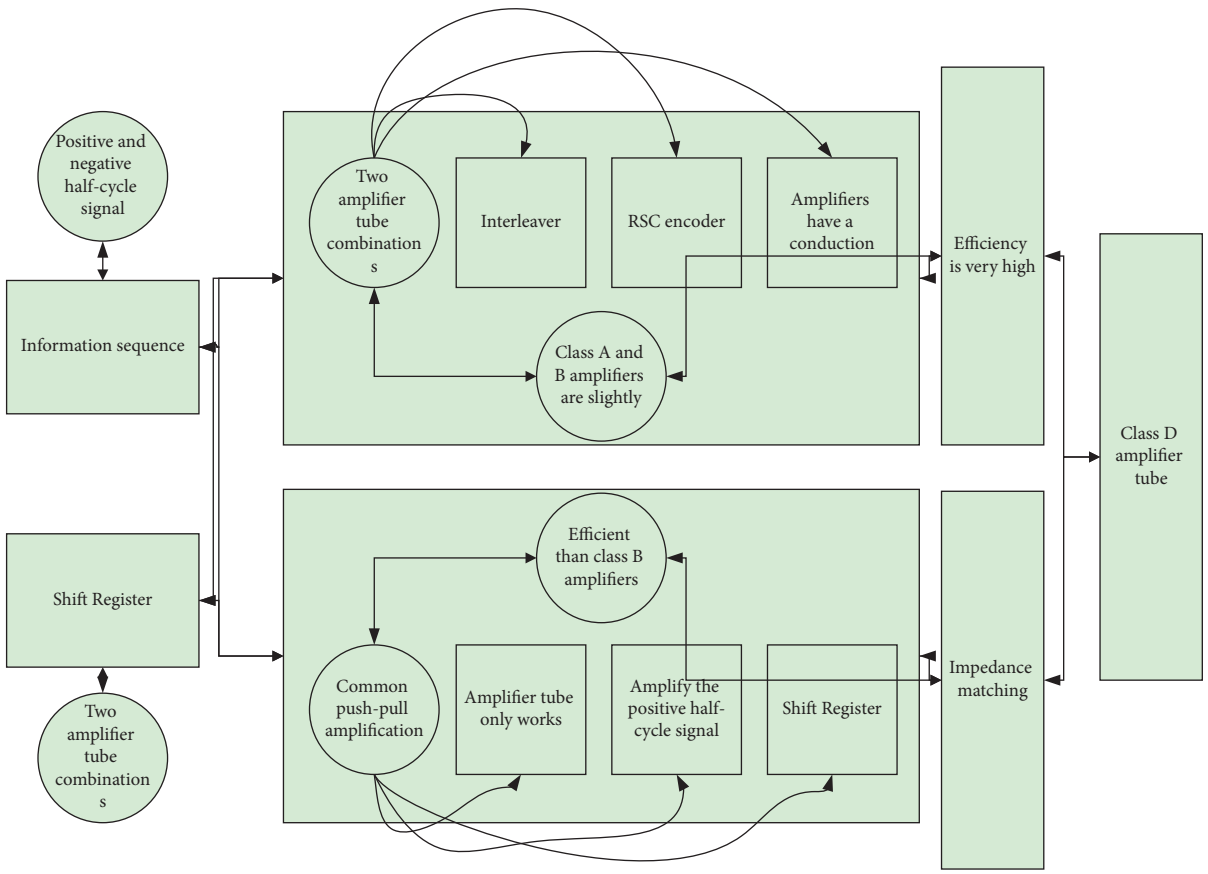

Figure 4: Parallel cascaded convolutional code encoder.

extracting information systems and recursive bits that can ensure that the data reach the end-user terminal accurately. Figure 5 depicts a schematic diagram of a Turbo cyclotron encoder consisting of two separate interleaved encoders.

The two independent check information sequences enter into the two-component decoders respectively, and each subdecoder decodes the system information sequence and check information sequence respectively to get different soft

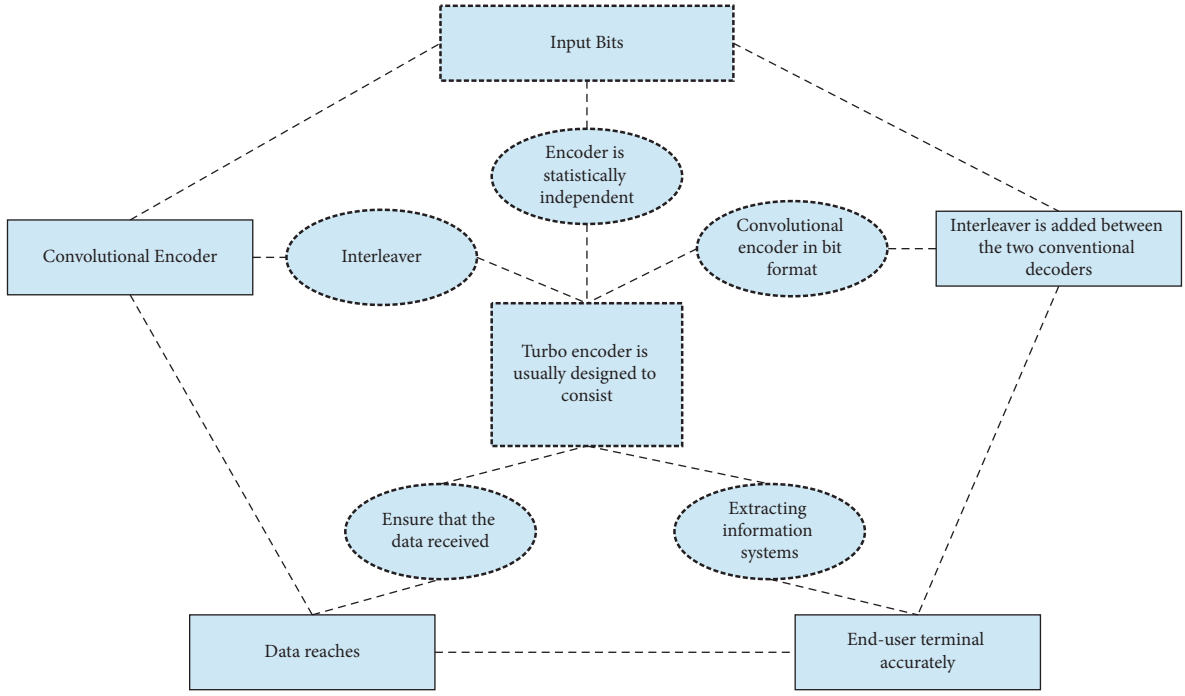

Figure 5: Structure of Turbo code encoder.

information about the information sequence, and then they exchange the relatively independent two sets of output soft information as to their respective new inputs, and after several iterations, the error bits in the received sequence are reduced to a certain degree, as well as the output soft information [16]. After several iterations, the error bits in the received sequence are reduced to a certain level, and the output soft information can be hard-judged as the decoded output so that a good error correction performance is achieved.

The encoded check bits are processed to produce codewords of different code rates. The component encoder can be either a recursive systematic convolution (RSC) code or a nonsystematic convolution (NSC) code. Given an RSC code, it is always possible to find an NSC code that generates polynomials corresponding to it and vice versa; see Figure 6 for the structure of the Turbo receiver of ISI channel.

Because the calculation of the forward state metric and backward state metric of each information bit in the log-map decoding algorithm of turbo code depends on serial recursive operations, the processing time of the whole decoding process increases significantly when using larger code blocks and interleaves that can bring better error correction performance, which causes significant processing delays and limits the channel compilation code rate [17]. When turbo coding is applied in a practical communication system, the turbo decoding algorithm needs to be improved by weighing the processing delay, system throughput, and hardware resource consumption. Common turbo decoding improvement structures include the sliding window decoding algorithm, block parallel decoding structure, and radix-8 algorithm.

An improved decoding method is to use sliding windows for decoding. The sliding window decoding algorithm divides a long block of code into multiple windows according to a preset window length and slides to each window in turn for decoding. In the processing of the sliding window algorithm, the initial values of the forward state metric and backward state metric of each window are used [18]. After analyzing the characteristics of Circular Permutation Code Words (CPC), taking the group interface of a communication private network as an example, the hardware circuit design scheme of the group CPC transceiver is introduced, and the generation of the CPC decoding table is given. The algorithm focuses on the module division, function and implementation method of the circuit, and the design and use of registers and briefly analyzes the detection performance of the circuit. The design is implemented by a field programmable logic device (FPGA), and the resource occupancy is low, has good portability, and can be used for similar interfaces after simple modification. It is a relatively common CPC transceiver circuit. By taking advantage of the convergence of the lattice recursive computation, the various unknown probabilities are in advance.

The basic structure of the Turbo code decoder is shown in Figure 7.

The hard judgment module is used to process the soft information of the final output of the second component decoder after several iterations to obtain the decoded output information bit sequence of the decoder [19].

4.3. Simulation Results for the Design of Turbo Code Coding Scheme in a High-Speed Hydroacoustic OFDM Communication. The simulation results of the Turbo code

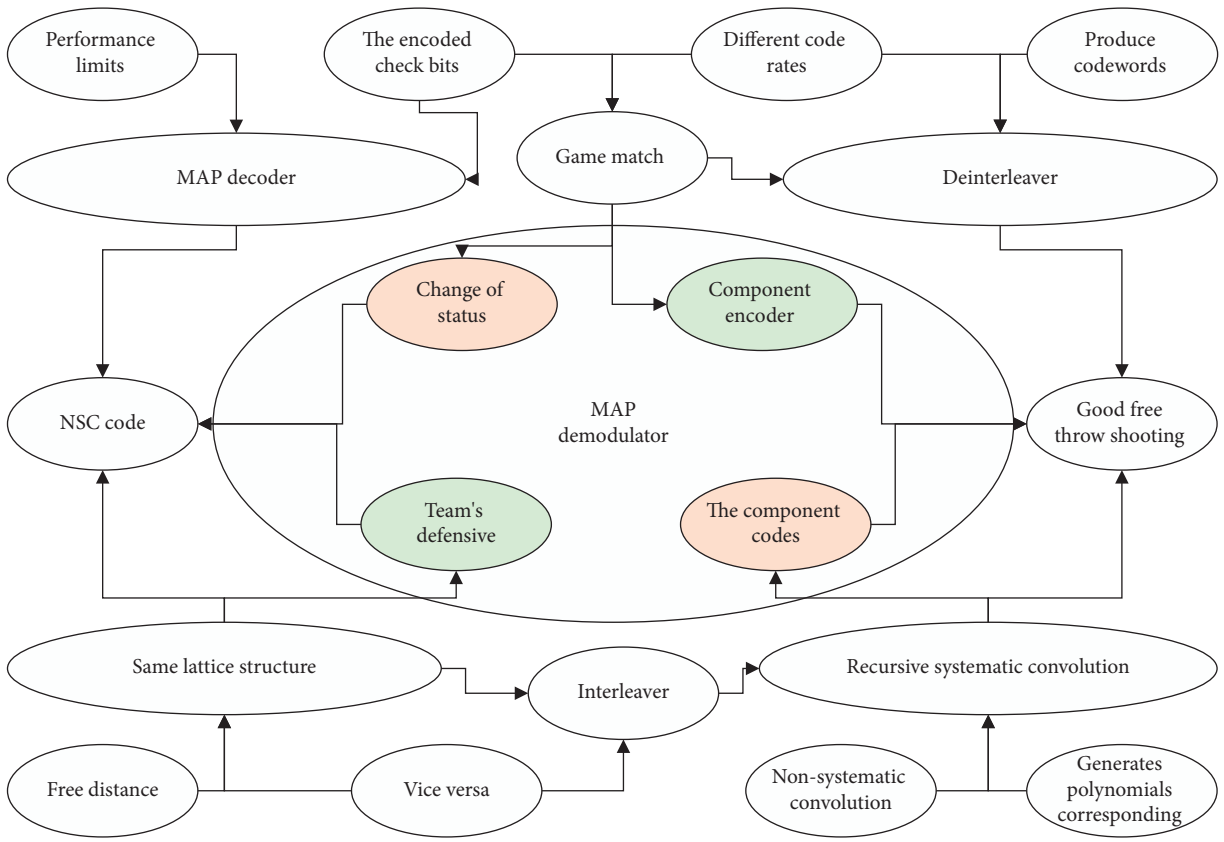

Figure 6: Turbo receiver architecture for ISI channel.

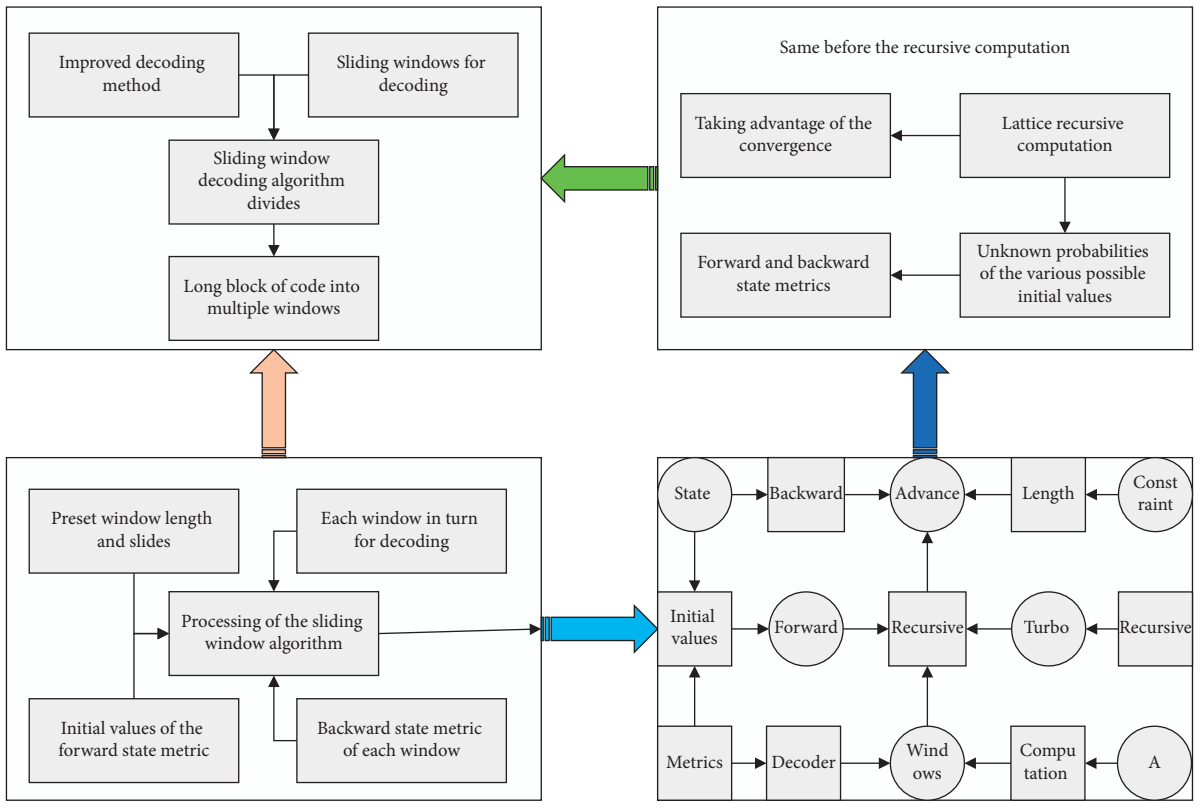

Figure 7: Block diagram of Turbo code iterative decoding structure.

coding scheme in high-speed hydroacoustic OFDM communication designed as described above are as follows. Per-packet BER, shown as a percentage packet error rate. For most of the packets, the BER is zero. See Figure 8 for simulation results of the high-speed hydroacoustic OFDM communication system based on Turbo codes, per packet BER.

When using the maximum frame length of N-6144 for turbo coding in the LTE standard, the decoding rate uses the fully parallel decoding algorithm. If shorter frame lengths are used, the decoding rate advantage of the fully parallel decoding algorithm decreases but is still much higher than that of the log-map algorithm. Although the fully parallel decoding algorithm can greatly increase the decoding rate and reduce the decoding latency, it will significantly increase the hardware resources required by the decode, and the fully parallel turbo decoder requires a large amount of computing and register resources. System sticks to LTE speed.

See Figure 9 for simulation results of high-speed hydroacoustic OFDM communication system based on Turbo codes-S/N ratio.

The fully parallel decoding algorithm with 36 iterations of approximate computation is shown in Figure 9 when a longer frame length of 4800 is used. The decoding performance of the max-log-map algorithm with 6 iterations and the fully parallel decoding algorithm with 36 iterations of approximate computation are very similar for different frame lengths.

Our system is relatively perfect, and it has almost no effect on the thermodynamics of water, so we do not need to consider the thermodynamics of water.

To avoid that the value of the state metric exceeds the range of the data bit width of the fixed-point quantization, which brings the decoder's error correction capability down, the hardware implementation adopts the method of normalizing the state metric to reduce the value of the forward and backward state metrics to ensure that they are limited to the range supported by the data quantization bit width. Within the range supported by the data quantization bit width, the backward and forward equalization of the received signal by the scatter plot gives an idea of the modulation being used by the system; see Figure 10 for simulation results of a high-speed hydroacoustic OFDM communication system based on unbalanced Turbo codes and Figure 11 for simulation results of a high-speed hydroacoustic OFDM communication system based on balanced Turbo codes.

The formation mechanism of multipath is again very different in shallow water environments, which consists of possible direct paths and reflections from the seafloor, and in deep water, which is caused by the bending of sound lines. The hydroacoustic communication in shallow sea channels is seriously affected by multipath effects and is prone to large impacts. In the shallow sea hydroacoustic communication, the sound velocity profile has a significant impact on the multipath effect, and Figure 10 gives several typical sound velocity profile cases. From the figure it can be seen that, in the sound velocity of the uniform sea, sound waves will reach the location of the receiving point through multiple surfaces

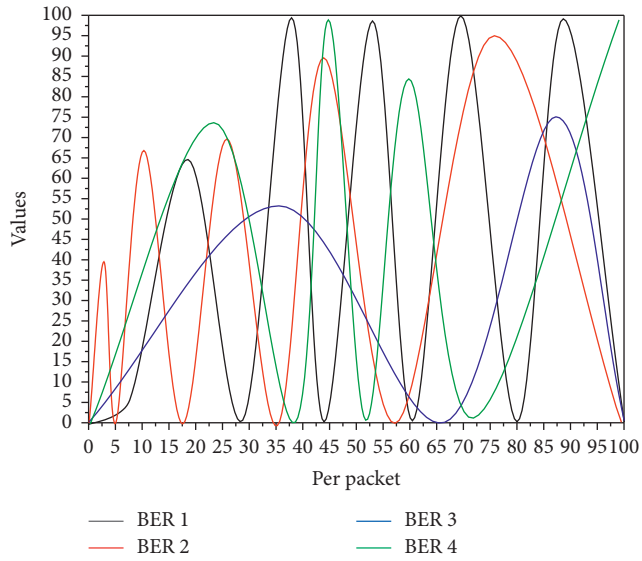

Figure 8: Simulation results of the high-speed hydroacoustic OFDM communication system based on Turbo codes, BER per packet.

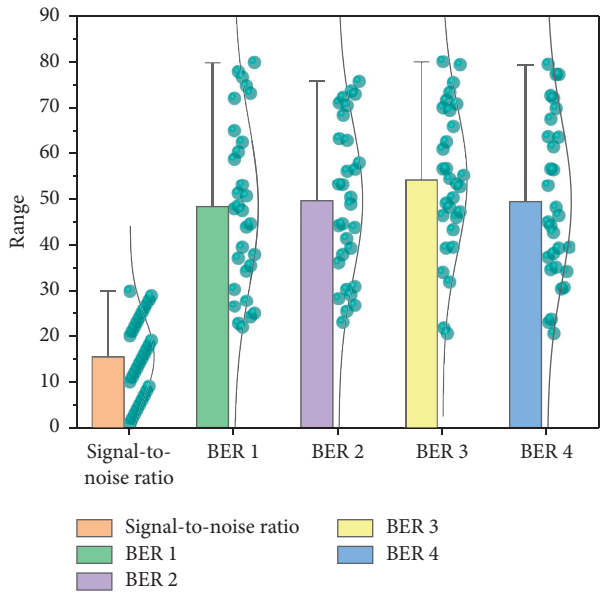

Figure 9: Simulation results of the high-speed hydroacoustic OFDM communication system based on Turbo codes-signal-to-noise ratio.

or seafloor reflections, and, in the negative gradient shallow sea, the seafloor reflection is the main mode of propagation, near the sound waves and can be reached through the straight line and surface path. In the long-distance, only part of the surface scattered signal and seafloor reflections can reach the location; for positive gradient shallow sea, sound waves reach the location of the receiving point. For positive gradient shallow sea, the acoustic wave reaches the location of the receiving point through multiple surface reflections.

The intercode interference caused by multipath seriously affects the performance of hydroacoustic communication

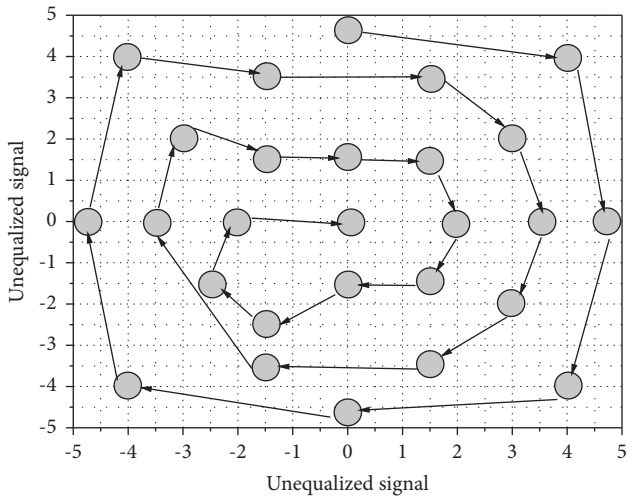

Figure 10: Simulation results of the high-speed hydroacoustic OFDM communication system based on unbalanced Turbo codes.

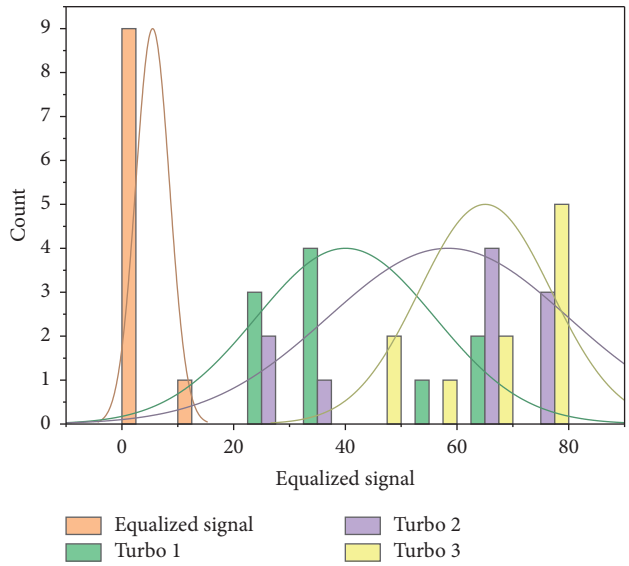

Figure 11: Simulation results of the high-speed hydroacoustic OFDM communication system based on balanced Turbo codes.

systems and causes great problems to ensure robust and high-speed hydroacoustic communication. The ISI in wireless communication is very short, often only a few code elements long. In contrast, the ISI of hydroacoustic communication is much larger, usually tens or even hundreds of code elements in length, which makes it more difficult or even impossible to distinguish the verdict at the receiving end. Therefore, to ensure robust and reliable hydroacoustic communication, the intercode interference caused by the multipath effect must be reduced or eliminated, and this is a major point and difficulty in the field of hydroacoustic communication.

For variables that are often applied throughout the algorithm, as well as input and output variables for DSP library functions used in the core algorithm, the storage location should be determined by the space they occupy. For example, allocate three segments of storage space for the operation of the DSP's built-in Fast Fourier Transform library function. The input and output arrays of the Fast Fourier Transform of length 16384 are stored in the form of alternating floating-point arrays, which occupy 13.1072 KB, so if all the input and output arrays of this function are allocated in the cache, the total space required is about 40 KB and should be placed in the L2 cache.

The SNR of the received signal can be estimated at the receiver side, and then the SNR of the received signal can be changed by adding additive Gaussian white noise, and the BER can be calculated under different SNRs, so the BER curve with SNR can be obtained, which is called the semisimulation experiment.

Figure 11 shows the BER performance comparison of the OFDM system with the precoding module, the black line shows the result of the semisimulation experiment without precoding at the transmitter, the rose line shows the result of the semisimulation experiment with ZF precoding at the transmitter, the green line shows the result of the semisimulation experiment with MMSE precoding at the transmitter, and the blue line shows the result of the semisimulation experiment with ZF-THP.

From Figure 11, after using the precoding technique at the transmitter side, only a simple detection process is required at the receiver side to achieve good performance. Moreover, the performance of the system with nonlinear precoding is better than that of the system with linear precoding.

The BER performance of the hydroacoustic STBC-SCFDE system with spatial and temporal diversity is better than that of the hydroacoustic SC-FDE system with a single transmitter and single receiver; in addition, the BER of the system decreases as the number of transmit antennas increases. The hydroacoustic STBC-SCFDE system is feasible and effective.

5. Conclusion

Through the above introduction of key technologies of high-speed hydroacoustic communication and the study of a hydroacoustic communication system with OFDM, the key technologies and advantages and disadvantages of OFDM application in a hydroacoustic communication system are analyzed, and a high-speed hydroacoustic OFDM communication coding scheme is designed based on TURBO codes. System simulation is conducted to analyze the data rate, unbalanced signal, balanced signal, received signal power spectrum, balanced signal power spectrum, the signal-to-noise ratio, bit rate, and per-packet BER results analyzed. Finally, the reliability of TURBO codes in high-speed hydroacoustic OFDM communication is analyzed with the simulation results of BER and SNR relationships under different conditions. Parametric modeling of the hydroacoustic OFDM system under impulsive noise interference is carried out. For the time domain impulse noise and large-amplitude single-frequency noise cancellation, a compression-aware technique is used, and the energy on the null

wave is used as a constraint for iterative cancellation of the time domain impulse noise and large-amplitude single-frequency noise, and the distributed cancellation method and the joint estimation cancellation method are compared. Simulation and experimental results show that the distributed cancellation method and the joint estimation cancellation method have good results for both time-domain impulse noise and large-amplitude single frequency noise cancellation, while the joint estimation cancellation method in which the large-amplitude single frequency noise cancellation is performed first has better performance.

Data Availability

The data used to support the findings of this study are available from the corresponding author upon request.

Conflicts of Interest

The authors declare that they have no conflicts of interest.

Acknowledgments

This work was supported by College of Physics and Electrical Engineering, Kashi University.

References

[1] M. Stojanovic, "Recent advances in high-speed underwater acoustic communication," *IEEE Journal of Oceanic Engineering*, vol. 21, no. 2, pp. 125–136P, 1996.

[2] M. Stojanovic and J. Preisig, "Underwater acoustic communication channels: propagation models and statistical characterization," *IEEE Communications Magazine*, vol. 47, no. 1, pp. 84–89, 2009.

[3] H. C. Song, W. A. Kuperman, and W. S. Hodgkiss, "Basin-scale time reversal communications," *Journal of the Acoustical Society of America*, vol. 125, no. 1, pp. 212–217, 2009.

[4] G. A. Jones, D. H. Layer, and T. G. Osenkowsky, "ETSI EN 301 701 digital video broadcasting (DVB); OFDM modulation for microwave digital terrestrial television," *Language Arts & Disciplines*, vol. 13, 2013.

[5] M. Chitre, S. Shahabodeen, and M. Stojanovic, "Under water acoustic communications and networking: recent advances and future challenges," *Marine Technology Society Journal*, vol. 42, no. 1, pp. 103–116, 2008.

[6] S. Roy, T. M. Duman, V. McDonald, and J. G. Proakis, "High-rate communication for underwater acoustic channels using multiple transmitters and space-time coding: receiver structures and experimental results," *IEEE Journal Oceanic engineering*, vol. 33, 2007.

[7] B. Li, S. Zhou, M. Stojanovic, L. Freitag, and P. Willett, "Multicarrier communication over underwater acoustic channels with non-uniform Doppler shifts. Oceanic engineering," *IEEE Journal of Oceanic Engineering*, vol. 33, pp. 110–112, 2008.

[8] E. F. Sang and S. K. Xu, "Turbo codes in hydroacoustic OFDM communication," *Journal of Harbin Engineering University*, vol. 30, no. 1, 2009.

[9] J.-G. Huang, H. Wang, C.-B. He, Q.-F. Zhang, and L.-Y. Jing, "Underwater acoustic communication and the general performance evaluation criteria," *Frontiers of Information Technology & Electronic Engineering*, vol. 19, no. 8, pp. 951–971, 2018.

[10] P. Chen, Y. Rong, S. Nordholm, and Z. He, "An underwater acoustic OFDM system based on NI CompactDAQ and LabVIEW," *IEEE Systems Journal*, vol. 13, no. 4, pp. 3858–3868, 2019.

[11] M. J. Bocus, A. Doufexi, and D. Agrafiotis, "Performance of OFDM-based massive MIMO OTFS systems for underwater acoustic communication," *IET Communications*, vol. 14, no. 4, pp. 588–593, 2020.

[12] G. Qiao, Z. Babar, L. Ma, and N. Ahmed, "Channel Estimation and Equalization of Underwater Acoustic MIMO-OFDM Systems: a Review Estimation du canal et l'égalisation des systèmes MEMS-MROF acoustiques sous-marins: une revue," *Canadian Journal of Electrical and Computer Engineering*, vol. 42, no. 4, pp. 199–208, 2019.

[13] Y. X. Yun-Xiang Guo, X.-A. Song, R.-Q. Zhang, and H. Li, "Research on underwater acoustic communication system based on OFDM-OAM," *Automatic Control and Computer Sciences*, vol. 54, no. 6, pp. 541–548, 2020.

[14] C.-F. Lin, H.-H. Lai, and S.-H. Chang, "MIMO GS OVSF/OFDM based underwater acoustic multimedia communication scheme," *Wireless Personal Communications*, vol. 101, no. 2, pp. 601–617, 2018.

[15] M. R. Khan, B. Das, and B. B. Pati, "Channel estimation strategies for underwater acoustic (UWA) communication: an overview," *Journal of the Franklin Institute*, vol. 357, no. 11, pp. 7229–7265, 2020.

[16] M. Y. I. Zia, P. Otero, and J. Poncela, "Design of a low-cost modem for short-range underwater acoustic communications," *Wireless Personal Communications*, vol. 101, no. 1, pp. 375–390, 2018.

[17] G. Qiao, Z. Babar, L. Ma, and X. Li, "Cost function based soft feedback iterative channel estimation in OFDM underwater acoustic communication," *Infocommunications Journal*, vol. 11, no. 1, pp. 29–37, 2019.

[18] C.-X. Wang, J. Huang, H. Wang, X. Gao, X. You, and Y. Hao, "6G wireless channel measurements and models: trends and challenges," *IEEE Vehicular Technology Magazine*, vol. 15, no. 4, pp. 22–32, 2020.

[19] M. Y. I. Zia, J. Poncela, and P. Otero, "State-of-the-art underwater acoustic communication modems: classifications, analyses and design challenges," *Wireless Personal Communications*, vol. 116, no. 2, pp. 1325–1360, 2021.